


# SCIENTIFIC REPORTS

OPEN

## Transport and Association of Ions in Lithium Battery Electrolytes Based on Glycol Ether Mixed with Halogen-Free Orthoborate Ionic Liquid

Faiz Ullah Shah<sup>1</sup>, Oleg I. Gnezdilov<sup>2</sup>, Rashi Gusain<sup>1</sup> & Andrei Filippov<sup>1,2</sup> 

Ion transport behaviour of halogen-free hybrid electrolytes for lithium-ion batteries based on phosphonium bis(salicylato)borate [P<sub>4,4,4,8</sub>][BScB] ionic liquid mixed with diethylene glycol dibutyl ether (DEGDDBE) is investigated. The Li[BScB] salt is dissolved at different concentrations in the range from 0.15 mol kg<sup>-1</sup> to 1.0 mol kg<sup>-1</sup> in a mixture of [P<sub>4,4,4,8</sub>][BScB] and DEGDDBE in 1:5 molar ratio. The ion transport properties of the resulting electrolytes are investigated using viscosity, electrical impedance spectroscopy and pulsed-Field Gradient (PFG) NMR. The apparent transfer numbers of ions are calculated from the diffusion coefficients measured by using PFG NMR. PFG NMR data suggested ion association upon addition of Li salt to the [P<sub>4,4,4,8</sub>][BScB] in DEGDDBE solution. This is further confirmed by liquid state <sup>7</sup>Li and <sup>11</sup>B NMR, and FTIR spectroscopic techniques, which suggest strong interactions between the lithium cation and oxygen atoms of the [BScB]<sup>-</sup> anion in the hybrid electrolytes.

The continuous emission of CO<sub>2</sub> into the atmosphere is thought to have catastrophic and irreversible effects on our planet such as rising of sea levels, acidification of oceans, polar melts, droughts, flood and global warming<sup>1</sup>. In this context, efficient electrical energy storage devices are highly desired in order to keep control on CO<sub>2</sub> emissions into the atmosphere. This is one of the main reasons for the growing interest in electrical energy storage devices for transportation technologies. In this context, lithium-ion batteries are attracting attentions of researchers due to their high energy density, acceptable cycle life, no memory effect and low self-discharging<sup>2</sup>. An electrolyte is a key component of lithium-ion batteries acting as an ionic conductor and electronic insulator. A desirable electrolyte should have the following properties<sup>3</sup>: (1) wide electrochemical window; (2) high ionic conductivity; (3) high chemical and thermal stability; (4) chemical inertness to other components of the cell such as electrodes, separator and the cell packing materials; (5) safe, non-toxic, economical and recyclable.

Extensive research efforts are being made to identify electrolytes that can perfectly meet the requirements of lithium-ion batteries. Despite the continuous research efforts, development of safe and efficient electrolytes remains a challenge. Ionic liquids (ILs) possess a combination of physicochemical properties such as high ionic conductivity, high chemical and electrochemical stability, non-flammability, non-volatility, high thermal stability, and wide liquid range<sup>4,5</sup>. ILs are salts composed of cations and anions that are liquids at or below 100 °C<sup>6</sup>. ILs are mixed with an appropriate lithium salt to make electrolyte for lithium-ion batteries. The unusual properties of IL electrolytes make them attractive alternatives compared to the conventional organic electrolytes. However, there are a number of drawbacks of IL electrolytes. For example, the high viscosity and cost of ILs need to be reduced in order to replace organic electrolytes with IL electrolytes in lithium-ion batteries<sup>7</sup>. Mixing ILs with organic solvents is one of the best options to not only reduce the high viscosity and cost of ILs but also improve the transport and electrochemical properties of electrolytes<sup>8-10</sup>. In addition, the conventional ionic liquid electrolytes contain anions with halogen atoms such as BF<sub>4</sub><sup>-</sup>, PF<sub>6</sub><sup>-</sup>, etc. Such anions are prone to hydrolysis in moisture conditions

<sup>1</sup>Chemistry of Interfaces, Luleå University of Technology, Luleå, SE-97187, Sweden. <sup>2</sup>Institute of Physics, Kazan Federal University, 420008, Kazan, Russia. Correspondence and requests for materials should be addressed to F.U.S. (email: [faisha@ltu.se](mailto:faisha@ltu.se)) or A.F. (email: [andrei.filippov@ltu.se](mailto:andrei.filippov@ltu.se))

and thus produce toxic and corrosive products limiting their applicability in batteries. Therefore, halogen-free IL electrolytes are necessary for high performance of the batteries and enhanced safety<sup>11,12</sup>.

Orthoborate-based salts are believed to be more efficient than the conventional salt such as LiPF<sub>6</sub> because they offer several advantages such as good thermal stability, high compatibility with cathode materials, no erosion of manganese and iron cathode materials, and are also halogen-free and non-toxic<sup>13,14</sup>. A variety of orthoborate-based lithium salts and their derivatives such as lithium bis[1,2-benzenediolato(2-)-O,O']borate Li[BBB]<sup>15</sup>, lithium bis[2,3-naphthalene-diolato(2-)-O,O']borate Li[BNNB]<sup>16</sup>, lithium bis[2,2-biphenyldiolato(2-)-O,O']borate Li[BBPB]<sup>17</sup>, lithium bis[croconato]borate Li[BCB]<sup>18</sup> and lithium bis(salicylato)borate Li[BScB]<sup>19,20</sup> have been studied in different organic solvents as electrolytes for lithium-ion batteries. Some of the commonly used organic solvents for orthoborate salts are ethylene carbonate (EC), propylene carbonate (PC), dimethyl carbonate (DMC), Diethyl carbonate (DEC), Ethyl sulfite (ES), Dimethyl sulfite (DMS), Diethyl sulfite (DES), gamma-butyrolactone, vinylene carbonate<sup>21–24</sup>. The main reason for the high ionic conductivity, wide electrochemical stability window and high thermal stability of orthoborate anions is their charge delocalization. Particularly, the aromatic orthoborate anions, also known as Hückel anions, are potential electrolytes for batteries as compared with the conventional salts<sup>25,26</sup>. A variety of lithium borate salts and their potential applications in high performance lithium batteries have been recently reviewed by Liu *et al.*<sup>27</sup>.

An appropriate organic solvent is critically important not only for the dissolution of lithium orthoborate salt but also for oxidative stability, thermal stability, satisfactory conductivity, cell performance and life cycle<sup>28</sup>. Ether based organic solvents (also known as glymes) are gaining attentions in lithium ion batteries due to a number of advantages such as low viscosity, high thermal stability and safety<sup>29,30</sup>. Recently, a number of studies have demonstrated that mixtures of ionic liquids and glymes possess excellent electrolyte properties and are promising solvents for lithium-ion batteries<sup>31–35</sup>.

In this paper, we explore the ion transport mechanism of ternary mixture of [P<sub>4,4,4,8</sub>][BScB] IL, diethylene glycol dibutyl ether (DEGDBe) and a Li[BScB] salt. DEGDBe has a flash point at 118 °C and high miscibility with [P<sub>4,4,4,8</sub>][BScB] IL. To the best of our knowledge, this is the first study on investigation of ion transport mechanism of orthoborate-based ionic liquid hybrid electrolytes. The Li[BScB] salt is dissolved in a mixture of [P<sub>4,4,4,8</sub>][BScB] IL and DEGDBe with different concentrations in the range from 0.15 mol kg<sup>-1</sup> to 1.0 mol kg<sup>-1</sup>. Electrical impedance spectroscopy (EIS) and PFG NMR spectroscopy (NMR diffusometry) are employed to understand the ion transport mechanism in the ternary mixtures. The physical and transport properties are investigated using ionic conductivity, viscosity, thermal analysis, multinuclear <sup>13</sup>C, <sup>31</sup>P, <sup>11</sup>B and <sup>7</sup>Li NMR spectroscopy, FTIR spectroscopy and NMR diffusometry.

## Experimental Section

**Materials.** Ionic liquid [P<sub>4,4,4,8</sub>][BScB] and Li[BScB] salt were synthesized as described in our previous publication<sup>36</sup>. The structure and purity of the products were confirmed by using <sup>1</sup>H, <sup>13</sup>C, <sup>31</sup>P and <sup>11</sup>B NMR spectroscopy. The samples were dried in a vacuum oven at 60 °C for more than 2 days before performing the experiments. As recently reported, the maximum solubility of Li[BScB] salt in [P<sub>4,4,4,8</sub>][BScB] IL is 0.418 mol kg<sup>-1</sup> (20 mol%)<sup>37</sup>. In this work, the electrolytes were prepared by mixing diethylene glycol dibutyl ether (DEGDBe) and [P<sub>4,4,4,8</sub>][BScB] IL in 5:1 molar ratio. Li[BScB] salt was dissolved in the DEGDBe (Sigma-Aldrich, purity ≥ 99%) and ionic liquid mixture in various concentration ranging from 0.15 mol kg<sup>-1</sup> to 1.0 mol kg<sup>-1</sup>. It is worth noting that the solubility of Li[BScB] salt is ca. 2.4 times higher in [P<sub>4,4,4,8</sub>][BScB] IL and DEGDBe mixture as compared with the neat [P<sub>4,4,4,8</sub>][BScB] IL. The chemical structures of DEGDBe and ionic components of [P<sub>4,4,4,8</sub>][BScB] IL are shown in Fig. 1.

The water content of the electrolytes was determined by Karl Fischer titration using 917 coulometer (Metrohm). The reported values are average of three independent measurements with standard deviation (SD). The water content of neat DEGDBe and [P<sub>4,4,4,8</sub>][BScB] IL were found to be 0.044 ± 0.001% and 0.039 ± 0.002%, respectively Table 1. The composition and water content of the hybrid electrolytes are shown in Table 1.

**NMR Spectroscopy.** The lithium salt and ionic liquid were characterized using Bruker Ascend Aeon WB 400 (Bruker BioSpin AG, Fällanden, Switzerland) NMR spectrometer. NMR spectra of the electrolytes were recorded with CDCl<sub>3</sub> solvent as an external lock. The working frequency was 100.63 MHz for <sup>13</sup>C, 162.01 MHz for <sup>31</sup>P, 128.40 MHz for <sup>11</sup>B and 155.56 MHz for <sup>7</sup>Li. Data were processed using Bruker Topspin 3.5 software.

**NMR Diffusometry.** NMR diffusion measurements were carried out on a Bruker Avance III (Bruker BioSpin AG, Fällanden, Switzerland) NMR spectrometer using PFG NMR probe Diff50 (Bruker) with a maximum amplitude of the magnetic field gradient pulse of 30 T m<sup>-1</sup>. The working frequencies for <sup>1</sup>H and <sup>7</sup>Li were 400.27 MHz and 155.56 MHz, respectively. For each NMR experiment, the sample was placed in a 5 mm glass tube and closed with a plastic stopper to avoid contact with air. The sample was equilibrated at a specific temperature for at least 30 min prior to measurements.

The detailed description of PFG NMR technique for measurement of molecular diffusion coefficients is reported earlier<sup>38</sup>. The primary information for the diffusion can be obtained from the diffusion decay (DD) of the NMR stimulated echo amplitude *A*. Diffusion decay of *A* for the stimulated echo pulse sequence in the case of simple non-associating molecular liquid can be described by the following equation<sup>39</sup>:

$$A(g, \delta, t_d) = A(0)\exp(-\gamma^2 g^2 \delta^2 D t_d) \quad (1)$$

where *A*(0) is a factor proportional to the proton content in the system and is dependent on the spin-lattice and spin-spin relaxation times,  $\gamma$  is the gyromagnetic ratio for a specific nucleus; *g* and  $\delta$  are the amplitude and

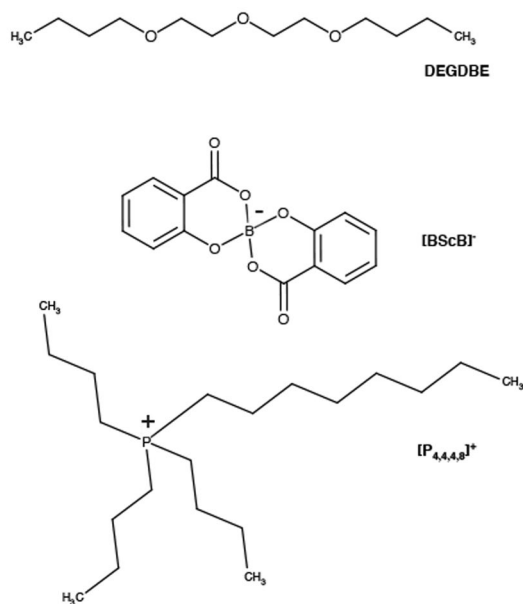


**Figure 1.** Structures and abbreviations of diethylene glycol dibutyl ether (DEGDBE) and tributylmethylphosphonium [P<sub>4,4,4,8</sub>]<sup>+</sup> cation and bis(salicylato)borate anion [BScB]<sup>-</sup> of the ionic liquid.

Li[BScB] concentration (mol kg <sup>-1</sup> )	Molar ratio			Water content (%) ± SD
	DEGDBE	[P <sub>4,4,4,8</sub> ][BScB]	Li[BScB]	
0	5	1	0	0.163 ± 0.003
0.15	5	1	0.25	0.584 ± 0.013
0.30	5	1	0.5	0.614 ± 0.016
0.60	5	1	1.0	1.016 ± 0.040
0.90	5	1	1.5	1.325 ± 0.046
1.0	5	1	1.75	1.416 ± 0.054

**Table 1.** Composition and water content of the hybrid electrolytes investigated in this study.

duration of the gradient pulse;  $t_d$  is a diffusion time; and  $D$  is the self-diffusion coefficient. In our experiments,  $t_d$  was in the range 4–100 ms for <sup>1</sup>H diffusion, while  $t_d$  was in the range 200–700 ms for <sup>7</sup>Li diffusion.

**Ionic Conductivity.** The measurements of ionic conductivity of the electrolytes were carried out using Metrohm Autolab PGSTAT302N electrochemical workstation with FRA32M module for impedance measurements. A frequency range from 1 Hz to 1 MHz with an AC voltage amplitude of 50 mV<sub>rms</sub> was used for the measurements. About 70 μL of the electrolyte sample was placed in a TSC70 closed cell (70 μL solvent) from RHD instruments. The experiments were performed in temperature range from –20 °C to 100 °C within an uncertainty of ± 0.1 °C. A two-electrode setup was used: the Pt-wire with a diameter of 0.25 mm as a working electrode and a 70 μL platinum crucible as a sample container and a counter electrode. Prior to each measurement, both the electrodes were polished with a Kemet diamond paste 0.25 μm. The cell constant (K<sub>cell</sub> = 17.511 cm<sup>-1</sup>) was used for each experiment. The TSC70 closed cell was thermally equilibrated for at least 20 min before performing each experiment.

**Cyclic Voltammetry.** Cyclic voltammetry (CV) experiments were performed using Autolab potentiostat PGSTAT302N (Metrohm) in a closed sample container in air. About 70 μL of the electrolyte was placed in a sealed RHD instruments Microcell HC. Experiments were carried out at 20 °C temperature using 0.1 M tetrabutylammonium hexafluorophosphate as a supporting electrolyte. A three electrode setup was used: Pt crucible worked as a counter electrode, glass sealed Pt wire acted as a working electrode and Ag/AgCl electrode was used as a reference electrode, to perform the experiments. Both the counter and working electrodes were polished with a Kemet diamond paste 0.25 μm prior to each measurement. All the CVs were recorded with a scan speed of 100 mV s<sup>-1</sup>. The potential of reference electrode was determined using ferrocene as an internal standard. The CV measurements are reported versus Li/Li<sup>+</sup> redox couple reference potential (–3.04 V vs SHE). The values of potential against Li/Li<sup>+</sup> were placed on reference scale by evaluating the formal potential of ferrocene (0.532 V vs SHE, 3.572 V vs Li/Li<sup>+</sup>).

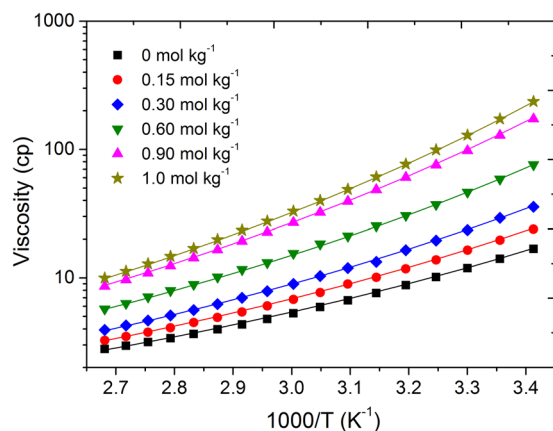


**Figure 2.** Dynamic viscosity of  $[P_{4,4,4,8}][BScB]$  IL based hybrid electrolytes. Symbols indicate the experimentally measured values and solid lines present best the fittings using VFT equation (2) with parameters of Table 2.

Li[BScB] concentration (mol kg <sup>-1</sup> )	$\eta_0^*$ , cp	$B$	$T_0$ , K	$E_\eta$ , kJ/(mol·K)
0	0.165	570	170	4.7
0.15	0.145	630	170	5.2
0.30	0.123	700	170	5.8
0.60	0.105	810	170	6.7
0.90	0.085	940	170	7.8
1.0	0.075	990	170	8.2

**Table 2.** VFT equation parameters and activation energies for viscosity data of  $[P_{4,4,4,8}][BScB]$  IL based hybrid electrolytes.

**Infrared Spectroscopy.** Fourier Transform Infrared (FTIR) spectra were recorded by applying a thin film of electrolyte on the KBr pellet using Bruker IFS 80 v vacuum fourier transform infrared spectrometer equipped with a deuterated triglycine sulphate (DTGS) detector. The experiments were carried out at room temperature ( $\sim 22^\circ\text{C}$ ) using the double side forward-backward acquisition mode. The total number of scans were 256 and signal-averaged at an optical resolution of  $4\text{ cm}^{-1}$ .

## Results and Discussion

The dynamic viscosity of  $[P_{4,4,4,8}][BScB]$  IL based hybrid electrolytes with various concentrations of Li[BScB] salt is shown in Fig. 2. The viscosity of  $[P_{4,4,4,8}][BScB]$  is significantly reduced when mixed with DEGDBE at 1:5 molar ratio. For example, the viscosity of the mixture of  $[P_{4,4,4,8}][BScB]$  and DEGDBE (1:5 molar ratio) is 1.25 cP at  $20^\circ\text{C}$  temperature, while the viscosity of neat  $[P_{4,4,4,8}][BScB]$  IL is 1400 cP at the same temperature<sup>36</sup>. It is clearly seen that viscosity increases with increase in the concentration of lithium salt and decreases rapidly with increase in temperature. As it is observed earlier for other hybrid electrolytes, the viscosity values of  $[P_{4,4,4,8}][BScB]$  IL based hybrid electrolytes follow Vogel-Fulcher-Tammann (VFT) behaviour as well<sup>40</sup>.

$$\eta = \eta_0^* \exp\left(\frac{B}{T - T_0}\right) \quad (2)$$

where  $\eta_0^*$ ,  $B$ , and  $T_0$  are the fitting parameters: pre-exponential factor, a factor related to the activation energy and the ideal glass transition temperature, respectively.  $T_0$  indicates a temperature at which free volume and mobility is reduced to zero<sup>41</sup>. The fitting procedure was performed in two steps, as previously reported<sup>37</sup>. In the first step,  $\ln(\eta)$  was plotted against  $1/(T - T_0)$  and selected  $T_0$  to have this dependence linear. The uncertainty in this step was  $\pm 10\text{ K}$ . In the second step, the dependence was fitted by a linear regression to obtain the fitting parameters ( $\eta_0^*$ ,  $B$ ). Activation energy for viscosity is related with  $B$  as  $E_\eta = B \cdot R$ , where  $R$  is a gas constant. The VFT equation parameters and activation energies for viscosity data are tabulated in Table 2.

The ionic conductivity of the hybrid electrolyte with various concentration of Li[BScB] salt is shown in Fig. 3. Unlike viscosity, no significant change is observed in the ionic conductivity when  $[P_{4,4,4,8}][BScB]$  is mixed with DEGDBE at 1:5 molar ratio. For example, the ionic conductivity of the mixture of  $[P_{4,4,4,8}][BScB]$  and DEGDBE (1:5 molar ratio) mixture is found to be  $7.3 \times 10^{-5}\text{ S cm}^{-1}$  and  $5.8 \times 10^{-4}\text{ S cm}^{-1}$  at  $20^\circ\text{C}$  and  $100^\circ\text{C}$  temperatures, respectively. While the ionic conductivity obtained for neat  $[P_{4,4,4,8}][BScB]$  IL is  $3.3 \times 10^{-5}\text{ S cm}^{-1}$  at  $20^\circ\text{C}$  and  $1.1 \times 10^{-3}\text{ S cm}^{-1}$  at  $100^\circ\text{C}$  temperature<sup>37</sup>. The higher ionic conductivity of the neat  $[P_{4,4,4,8}][BScB]$  IL at  $100^\circ\text{C}$  temperature reveals efficient dissociation of ions at higher temperature. On the contrary, the ions remain together in the mixture of  $[P_{4,4,4,8}][BScB]$  IL and DEGDBE even at higher temperature. The ionic conductivity decreases with

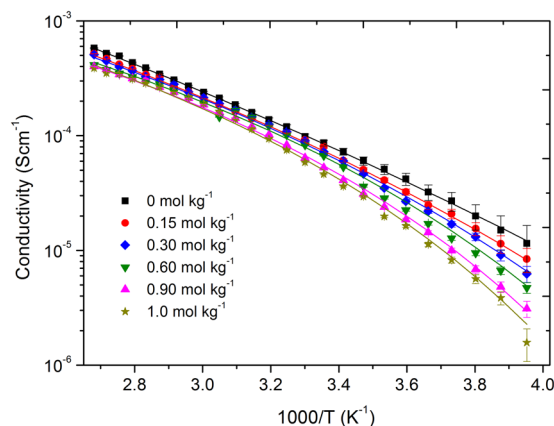


**Figure 3.** Ionic conductivity of  $[P_{4,4,4,8}][BScB]$  IL based hybrid electrolytes and their best fittings using VFT equation. Symbols indicate the experimentally measured values and solid lines present the best fittings using VFT equation (3) with parameters of Table 3.

Li[BScB] concentration (mol kg <sup>-1</sup> )	$\sigma_0^*$	$B$	$T_0$ , K	$E_\sigma$ , kJ/(mol·K)
	S/cm			
0	0.15	1630	80	13.6
0.15	0.047	1150	120	9.6
0.30	0.027	940	140	7.8
0.60	0.014	740	160	6.2
0.90	0.012	690	170	5.7
1.0	0.015	730	170	6.1

**Table 3.** VFT equation parameters and activation energies for ionic conductivity data of  $[P_{4,4,4,8}][BScB]$  IL based hybrid electrolytes.

the increase in the concentration of Li salt and it increases with increase in temperature for all the electrolytes studied. The addition of Li[BScB] salt causes an increase in viscosity and decrease in ionic conductivity of the electrolytes due to stronger coulombic interactions between the smaller lithium ions and the  $[BScB]^-$  anions as compared with the interactions between the larger phosphonium cations and the  $[BScB]^-$  anions<sup>42,43</sup>. The VFT equation is for ionic conductivity is<sup>40</sup>:

$$\sigma = \sigma_0^* \exp\left(\frac{-B}{T - T_0}\right) \quad (3)$$

where  $\sigma_0^*$ ,  $B$ , and  $T_0$  are the fitting parameters. The fitting procedure was performed as in the case of viscosity. The temperature dependence of ionic conductivity for  $[P_{4,4,4,8}][BScB]$  IL based hybrid electrolytes with different concentrations of Li[BScB] salt fit well to the VFT model over the entire temperature range studied. The VFT parameters for the ionic conductivity are tabulated in Table 3.

Diffusion decays for DEGDBE,  $[P_{4,4,4,8}]^+$ ,  $[BScB]^-$ , and  $Li^+$  were easily measured in the dynamic range of 2–3 decimal orders. Therefore, the achieved uncertainties in diffusion coefficients did not exceed 4.5%. This was estimated from the distribution of points in diffusion decays and also from the reproducibility values of diffusion coefficients in a consequent series of measurements. Figures 4 and 5 present the Arrhenius plots of diffusion coefficients of  $[P_{4,4,4,8}]^+$  and  $[BScB]^-$  (Fig. 4a), DEGDBE (Fig. 4b) and  $Li^+$  (Fig. 5). The diffusion data demonstrate a monotonous increase in diffusivities of  $[P_{4,4,4,8}]^+$ ,  $[BScB]^-$ , DEGDBE and  $Li^+$  with increase in temperature. Diffusion coefficients of DEGDBE are higher by a factor of 4–6 as compared with the ions of the IL and  $Li^+$ , while the diffusivities of ions in the IL and  $Li^+$  are comparable. As in the case of ionic conductivity, increase in the concentration of Li[BScB] lead to monotonous decrease in mobilities of all the four species present in the hybrid electrolyte system. Temperature dependences for  $[P_{4,4,4,8}]^+$ ,  $[BScB]^-$  and DEGDBE can be described by Arrhenius dependence for diffusion:

$$D(T) = D_0^* \cdot \exp\left(\frac{-E_D}{RT}\right) \quad (4)$$

where  $D_0^*$  is a parameter that is independent of temperature,  $E_D$  is the apparent molar activation energy of diffusion. Fitting parameters for diffusion of  $[P_{4,4,4,8}]^+$ ,  $[BScB]^-$  and DEGDBE are presented in Table 4. Arrhenius function shows a linear dependence in Arrhenius coordinates. However, this is not the case for the diffusion of

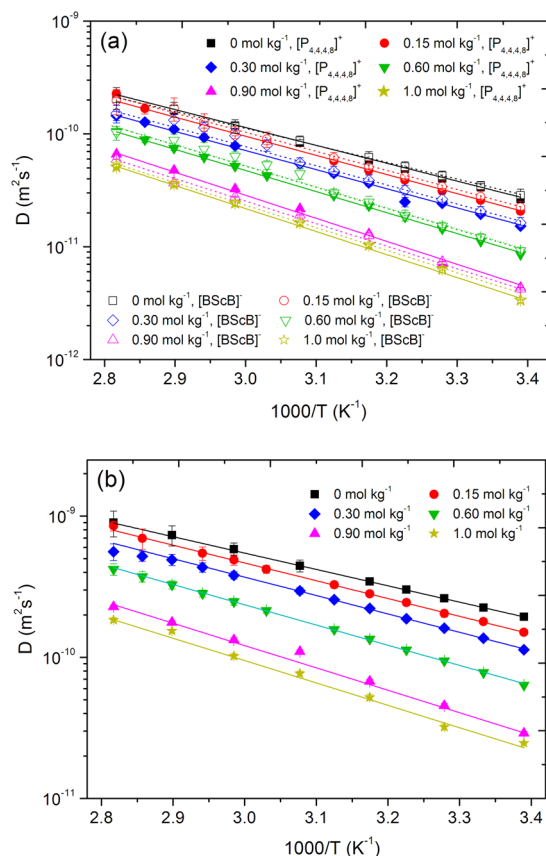


**Figure 4.** Arrhenius plot of diffusion coefficients of  $[P_{4,4,4,8}]^+$  cation,  $[BScB]^-$  anion and DEGDBE in the ionic liquid based hybrid electrolytes and their best fittings using Arrhenius type (4). The error bars are contained within the size of the points.

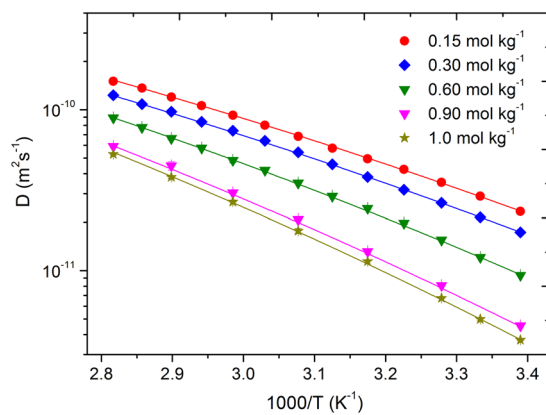


**Figure 5.** Arrhenius plot of diffusion coefficients of  $Li^+$  cation in the ionic liquid based hybrid electrolytes and their best fittings using VFT type equation (5). The error bars are contained within the size of the points.

$Li^+$  ions (Fig. 5). The universal form of temperature dependences of diffusion coefficients is the VFT equation in a form for diffusivity, which is equivalent to the Arrhenius dependence in the high-temperature limit<sup>40,43</sup>:

$$D = D_0^* \exp\left(\frac{-B}{T - T_0}\right) \quad (5)$$

where  $D_0^*$ ,  $T_0$ ,  $B$  are fitting parameters. Apparent energy of activation for diffusion is related with  $B$  as  $E_D = B \cdot R$ . We have described  $D(T)$  in Fig. 5 by fitting  $D_0^*$ ,  $T_0$  and  $B$ . Again, as in cases of viscosity and conductivity, the procedure of fitting was performed in two steps. The best fitting results are shown by solid lines in the Fig. 5 and the

Li[BScB] concentration (mol kg <sup>-1</sup> )	Diffusing component	$D_0$ , m <sup>2</sup> /s	$B$	$T_0$ , K	$E_D$ , kJ/(mol·K)
0	DEGDBe	$1.65 \times 10^{-6}$			22.2
	[P <sub>4,4,4,8</sub> ] <sup>+</sup>	$6.5 \times 10^{-6}$			30.3
	[BScB] <sup>-</sup>	$3.5 \times 10^{-6}$			28.7
0.15	DEGDBe	$2.8 \times 10^{-6}$			24.1
	[P <sub>4,4,4,8</sub> ] <sup>+</sup>	$11.5 \times 10^{-6}$			32.4
	[BScB] <sup>-</sup>	$12.5 \times 10^{-6}$			32.4
	Li <sup>+</sup>	$2.65 \times 10^{-8}$	1160	130	9.64
0.3	DEGDBe	$3.0 \times 10^{-6}$			24.9
	[P <sub>4,4,4,8</sub> ] <sup>+</sup>	$8.6 \times 10^{-6}$			32.4
	[BScB] <sup>-</sup>	$9.3 \times 10^{-6}$			32.4
	Li <sup>+</sup>	$2.65 \times 10^{-8}$	1210	130	10
0.6	DEGDBe	$4.7 \times 10^{-6}$			27.4
	[P <sub>4,4,4,8</sub> ] <sup>+</sup>	$19.0 \times 10^{-6}$			35.8
	[BScB] <sup>-</sup>	$21.0 \times 10^{-6}$			35.8
	Li <sup>+</sup>	$4.3 \times 10^{-8}$	1390	130	11.6
0.90	DEGDBe	$6.9 \times 10^{-6}$			30.3
	[P <sub>4,4,4,8</sub> ] <sup>+</sup>	$3.8 \times 10^{-5}$			39.1
	[BScB] <sup>-</sup>	$2.5 \times 10^{-5}$			38.2
	Li <sup>+</sup>	$7.3 \times 10^{-8}$	1600	130	13.3
1.0	DEGDBe	$5.4 \times 10^{-6}$			30.3
	[P <sub>4,4,4,8</sub> ] <sup>+</sup>	$2.9 \times 10^{-5}$			39.1
	[BScB] <sup>-</sup>	$2.3 \times 10^{-5}$			38.2
	Li <sup>+</sup>	$8.7 \times 10^{-8}$	1660	130	13.8

**Table 4.** The parameters of Arrhenius equation (4) and VFT equation (5), and activation energy for diffusion data for ionic liquid based hybrid electrolytes (Figs 4 and 5).

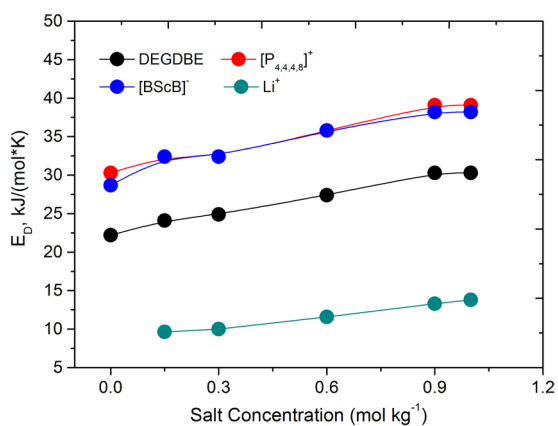


**Figure 6.** Apparent activation energy for diffusion of [P<sub>4,4,4,8</sub>]<sup>+</sup> cation, [BScB]<sup>-</sup> anion, DEGDBe and Li<sup>+</sup> cation in the ionic liquid based hybrid electrolytes.

corresponding fitting parameters are tabulated in Table 4. Apparent energy of activation ( $E_D$ ) for diffusive motion of DEGDBe is always a factor  $\sim 1.3$  lower as compared with the  $E_D$  of [P<sub>4,4,4,8</sub>]<sup>+</sup> and [BScB]<sup>-</sup>. The difference in  $E_D$  observed for diffusion of [P<sub>4,4,4,8</sub>]<sup>+</sup>, [BScB]<sup>-</sup> and Li<sup>+</sup> is conditioned by the difference in  $T_0$ . Increase in concentration of Li[BScB] in the electrolyte system leads to an increase in  $E_D$  of all four species. A graphical representation of  $E_D$  for all four species as a function of Li[BScB] salt is shown in Fig. 6 and the  $E_D$  values are tabulated in Table 4.

The decrease in diffusion coefficients with an increase in Li[BScB] salt suggests that the added lithium ions increase the sizes of diffusing entities in the hybrid electrolyte. Indeed, the small Li<sup>+</sup> ion diffuses with the same diffusion coefficient as the bulky [BScB]<sup>-</sup> and [P<sub>4,4,4,8</sub>]<sup>+</sup> ions. It means that the degree of dissociation of Li[BScB] is not very high and Li<sup>+</sup> ions diffuse together with the [BScB]<sup>-</sup> anion. This may happen if [P<sub>4,4,4,8</sub>]<sup>+</sup>, [BScB]<sup>-</sup> and Li<sup>+</sup> ions form associates, which present a diffusive entity in the hybrid electrolyte. It is worth noting that size of these associates increases as the concentration of Li[BScB] in the electrolyte system increases. The plausible explanation of this is stronger interactions between Li<sup>+</sup> cation and [BScB]<sup>-</sup> as compared with the interactions between [P<sub>4,4,4,8</sub>]<sup>+</sup> cation and [BScB]<sup>-</sup> anion. The increase in viscosity (Fig. 2) and decrease in ionic conductivity

Li[BScB] concentration (mol kg <sup>-1</sup> )	295 K			325 K			355 K		
	$t_{\text{Li}}$	$t_{[\text{P}_{4,4,4,8}]^+}$	$t_{[\text{BScB}]^-}$	$t_{\text{Li}}$	$t_{[\text{P}_{4,4,4,8}]^+}$	$t_{[\text{BScB}]^-}$	$t_{\text{Li}}$	$t_{[\text{P}_{4,4,4,8}]^+}$	$t_{[\text{BScB}]^-}$
0		0.482	0.518		0.490	0.510		0.508	0.492
0.15	0.005	0.474	0.521	0.005	0.478	0.518	0.004	0.532	0.465
0.30	0.011	0.472	0.517	0.010	0.484	0.506	0.008	0.479	0.523
0.60	0.021	0.461	0.518	0.018	0.428	0.555	0.017	0.488	0.495
0.90	0.015	0.476	0.492	0.031	0.501	0.469	0.028	0.496	0.475
1.0	0.015	0.462	0.500	0.038	0.458	0.505	0.035	0.450	0.514

**Table 5.** Apparent transference numbers of individual ions at various temperatures for the ionic liquid based hybrid electrolytes.

(Fig. 3) with the addition of lithium salts can be also explained by the increase in sizes of the diffusing entities in the hybrid electrolyte.

The apparent transference numbers of the ions were calculated from the self-diffusion coefficients using the following equation, as reported previously in a number of publications<sup>44,45</sup>.

$$t_i = \frac{x_i D_i}{\sum_j x_j D_j} \quad (6)$$

where  $t_i$  is the apparent transference number,  $x_i$  is the molar fraction of an ion and  $D_i$  is the self-diffusion coefficient of an ion in  $\text{m}^2\text{s}^{-1}$ . The apparent transference numbers of  $\text{Li}^+$ ,  $[\text{P}_{4,4,4,8}]^+$  and  $[\text{BScB}]^-$  ions for different concentrations and temperatures are presented in Table 5. As anticipated, the transference number of  $\text{Li}^+$  is significantly lower for electrolyte containing mixture of  $[\text{P}_{4,4,4,8}][\text{BScB}]$  and DEGDBE as compared to  $[\text{P}_{4,4,4,8}][\text{BScB}]$  based electrolyte without DEGDBE. For example, the transference number of  $\text{Li}^+$  in the hybrid electrolyte with lithium ion concentration of  $0.30 \text{ mol kg}^{-1}$  is 0.011 at 295 K, while it is 0.040 for  $[\text{P}_{4,4,4,8}][\text{BScB}]$  based electrolyte without DEGDBE under similar experimental conditions<sup>37</sup>. The apparent transference numbers of  $\text{Li}^+$  ion are lower in electrolyte containing mixture of  $[\text{P}_{4,4,4,8}][\text{BScB}]$  and DEGDBE as compared with  $[\text{P}_{4,4,4,8}][\text{BScB}]$  based electrolyte, although the concentration of lithium ion is 2.5 fold higher in the former electrolyte. The lower transference numbers of  $\text{Li}^+$  ion suggest that the ions are moving together in the form of clusters. Even the apparent transference numbers of the  $[\text{P}_{4,4,4,8}]^+$  cation and  $[\text{BScB}]^-$  anion are comparable with the  $[\text{P}_{4,4,4,8}][\text{BScB}]$  based electrolyte without DEGDBE. It reveals that the addition of DEGDBE did not affect the transference numbers of ions, however, the viscosity of the resulting electrolytes is significantly reduced.

There might be several reasons for the lower transference number of  $\text{Li}^+$  cation in the hybrid electrolytes. First, the  $\text{Li}^+$  cations could not be dissociated completely and form larger aggregates together with  $[\text{P}_{4,4,4,8}]^+$  cations and  $[\text{BScB}]^-$  anions that diffuse slowly in the electrolytes. It reveals that there are strong interactions between the  $\text{Li}^+$  cation and  $[\text{BScB}]^-$  anion. Second, the sizes of  $[\text{P}_{4,4,4,8}]^+$  cation and  $[\text{BScB}]^-$  anion are much larger than the typical ionic liquids comprising smaller cations such imidazolium and pyrrolidinium, and halogenated anions such as  $\text{BF}_4$ ,  $\text{PF}_6$  and  $\text{NTf}_2$ . The slower diffusivity is due to their large sizes and since lithium atom is strongly interacting with the anion, the mobility of lithium is affected as well. Third, it is known that PFG NMR method underestimates the diffusion coefficients of charged species. For example, Martins *et al.* have compared the calculated transference numbers of lithium ion in ILs using NMR diffusometry and electrochemical methods. It was found that the values calculated from electrochemical method were 2–3 fold larger as compared with the values determined from NMR diffusometry<sup>46</sup>. NMR diffusometry takes into account all the species and aggregates, which might be larger than the small charged  $\text{Li}^+$  cation and thus, underestimates the diffusion coefficients of the charged species.

In order to get deeper insights into the local environment, we performed  $^7\text{Li}$ ,  $^{11}\text{B}$ ,  $^{31}\text{P}$  and  $^{13}\text{C}$  NMR measurements of the electrolytes using  $\text{CDCl}_3$  as an external lock. As expected, significant changes in the chemical shifts of  $^7\text{Li}$  and  $^{11}\text{B}$  NMR spectra as a function of lithium salt concentration are observed (Figs 7 and 8). We did not observe any significant changes in the chemical shifts of the peaks for  $[\text{P}_{4,4,4,8}]^+$  cation in  $^{31}\text{P}$  and  $^{13}\text{C}$  NMR spectra recorded under the same experimental conditions (see ESI). However,  $^7\text{Li}$  NMR peaks shift towards lower ppm values with increasing Li salt concentration in the electrolyte. This significant change in chemical shift suggests that the chemical environment of  $\text{Li}^+$  ions is changing with increasing concentration of Li salt in the electrolyte. It reveals that the  $\text{Li}^+$  ions are more shielded upon addition of Li salt due to the stronger interactions between  $\text{Li}^+$  ions and  $[\text{BScB}]^-$  anions. This is in agreement with the earlier findings by Yoon, *et al.* in electrolytes based on LiFSI dissolved in  $\text{C}_3\text{mpyrFSI}$  ionic liquid; they have found that  $^7\text{Li}$  NMR spectra shift toward more negative values with increasing concentration of Li salt in the ionic liquid<sup>47</sup>. It is interesting to note that we observed similar changes towards lower ppm values in the  $^{11}\text{B}$  NMR spectra with increasing Li salt concentration as well (Fig. 8). This further confirms that addition of Li salt lead to stronger interactions between  $\text{Li}^+$  ions and  $[\text{BScB}]^-$  anions, which have shielded both lithium and boron nuclei.

A graphical representation of the changes in chemical shift and full width at maximum height (fwhm) as a function of Li salt concentration is shown in Fig. 9. A continuous shift towards lower ppm values is observed in the chemical shift of  $^7\text{Li}$  and  $^{11}\text{B}$  NMR spectra with addition of Li salt until it reaches the saturation point at  $1.0 \text{ mol kg}^{-1}$  concentration. Generally, the line width NMR peak increases with increasing Li salt concentrations and line width decreases with increasing temperature. Interestingly, we observed the opposite in the case of both  $^7\text{Li}$  and  $^{11}\text{B}$  NMR spectra of bis(salicylato)borate ionic liquid based hybrid electrolytes. The fwhm of  $^{11}\text{B}$  NMR



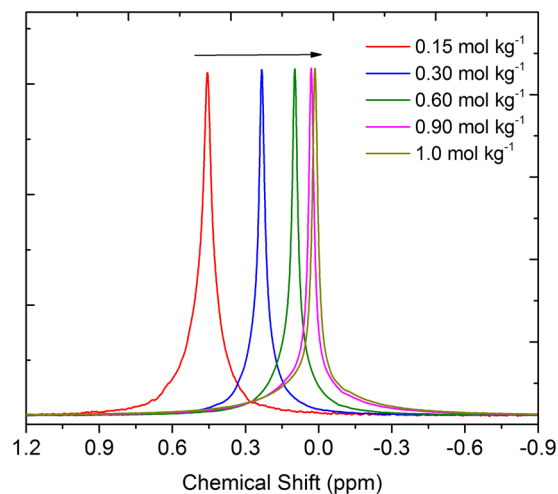


**Figure 7.**  $^7\text{Li}$  NMR spectra of  $[\text{P}_{4,4,4,8}][\text{BScB}]$  IL based hybrid electrolytes at 22 °C. 1 M LiCl was used as an external reference. Arrow indicates direction of increasing Li[BScB] salt concentration.

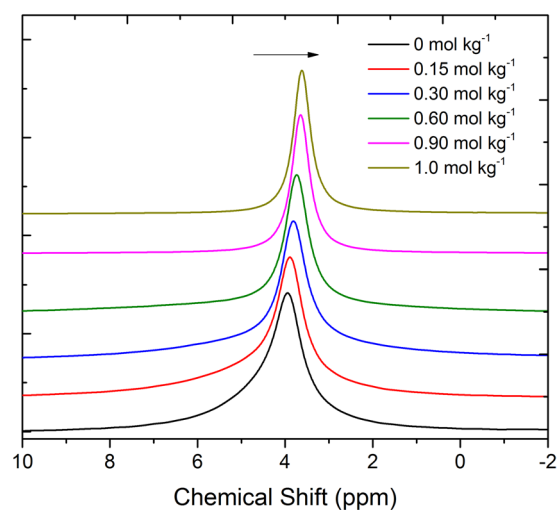


**Figure 8.**  $^{11}\text{B}$  NMR spectra of  $[\text{P}_{4,4,4,8}][\text{BScB}]$  IL based hybrid electrolytes at 22 °C. Arrow indicates direction of increasing Li[BScB] salt concentration.

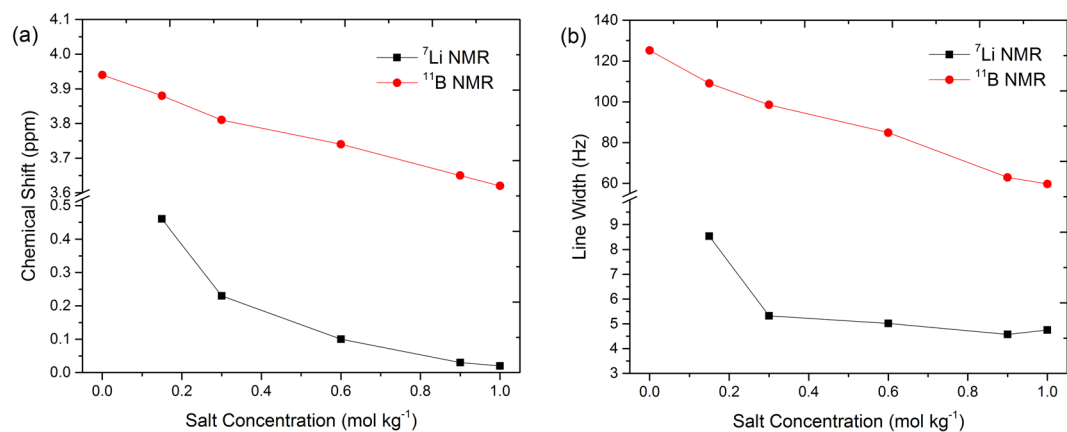


**Figure 9.** (a) Chemical shift and (b) line width of  $^7\text{Li}$  and  $^{11}\text{B}$  NMR spectra of  $[\text{P}_{4,4,4,8}][\text{BScB}]$  IL based hybrid electrolytes at 22 °C.

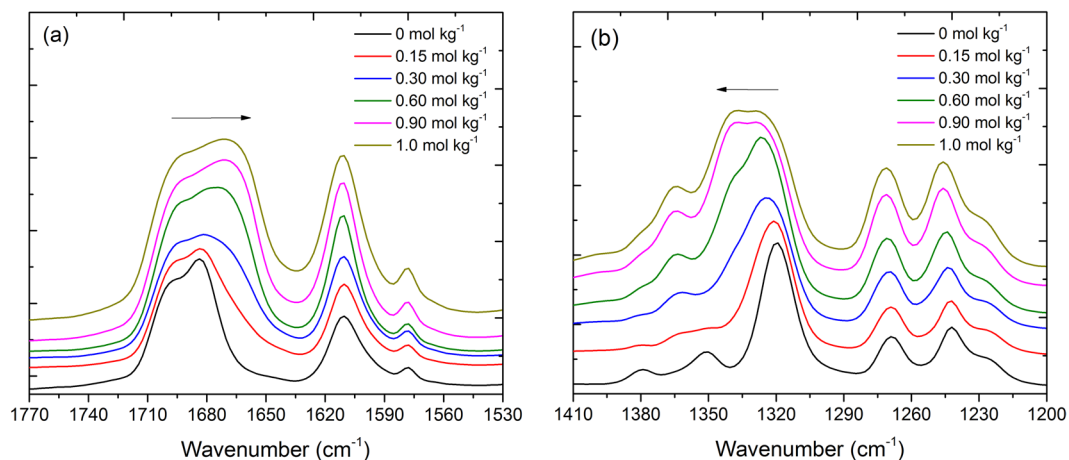


**Figure 10.** FTIR spectra of  $[P_{4,4,4,8}][BScB]$  IL based hybrid electrolytes in the frequency range (a) from  $1770\text{ cm}^{-1}$  to  $1530\text{ cm}^{-1}$  and (b) from  $1410\text{ cm}^{-1}$  to  $1200\text{ cm}^{-1}$ . Arrows indicate shift in wavenumber with increasing  $Li[BScB]$  salt concentrations.

spectra decreases continuously with increasing Li salt concentration, while in the case of  $^7Li$  NMR spectra a significant decrease is observed at  $0.15\text{ mol kg}^{-1}$  concentration of Li salt and then decreases slightly upon addition of more Li salt. However, the fwhm increases again slightly at Li salt concentration above  $0.90\text{ mol kg}^{-1}$ . The changes in line width reveal variation in ion dynamics as a function of Li salt concentration. Hilder *et al.* have recently observed a decrease in the line width of  $^{23}Na$  NMR spectra with increase in concentration of Na salt and increase with increase in temperature<sup>48</sup>. They have suggested that the signal shape is heavily affected by the quadrupolar interactions. In our case, both  $^7Li$  and  $^{11}B$  have comparable quadrupolar moments and both nuclei have spin 3/2.

Another explanation of the observed changes in  $^7Li$  and  $^{11}B$  NMR chemical shift and line width with  $Li^+$  concentration is related to the specific structure of a complex formed by  $Li^+$ ,  $[P_{4,4,4,8}]^+$  and  $[BScB]^-$  ions. With the increase in  $Li^+$  ion concentration, the concentration of  $[BScB]^-$  anions in the system remains unchanged but  $[P_{4,4,4,8}]^+$  cations are regularly being replaced by  $Li^+$  ions. The alteration of chemical shifts of  $^{11}B$  and  $^7Li$  but no changes in chemical shifts of  $^{31}P$  with increasing lithium salt concentration demonstrates selective changes in packing of ions in the complex concerning mainly  $Li^+$  and  $[BScB]^-$ . A decrease in line width is usually related with the decrease in transverse NMR relaxation rate ( $1/T_2$ ) and rotational correlation time of ions ( $\tau_c$ )<sup>49</sup>. Therefore, the decrease in line widths of  $^{11}B$  and  $^7Li$  NMR spectra is due to an increase in the rotational motion of  $Li^+$  and  $[BScB]^-$  ions because of replacement of the bulky  $[P_{4,4,4,8}]^+$  cations with the small  $Li^+$  ions.

FTIR spectroscopy was used to further investigate the interaction of  $Li^+$  ion with the  $[BScB]^-$  anion. The full FTIR spectra of bis(salicylato)borate ionic liquid based hybrid electrolytes with different concentrations of  $Li[BScB]$  salt are shown in ESI. Figure 10 shows selected regions of the FTIR spectra in the frequency range from  $1770\text{ cm}^{-1}$  to  $1530\text{ cm}^{-1}$  (Fig. 10a) and from  $1410\text{ cm}^{-1}$  to  $1200\text{ cm}^{-1}$  (Fig. 10b). The vibrations around  $1700\text{ cm}^{-1}$  are assigned to C=O stretching and around  $1610\text{ cm}^{-1}$  to the aromatic ring vibrations of  $[BScB]^-$  anion (Fig. 10a). As expected, the C=O band is shifted towards lower wavenumber values and peak broadening occurs upon addition of Li salt. This shift and broadening indicate the  $Li^+$  ion coordination with  $[BScB]^-$  anion. However, there is no change in the aromatic ring vibrations of  $[BScB]^-$  anion around  $1610\text{ cm}^{-1}$  with increasing lithium salt concentration.

The band around  $1320\text{ cm}^{-1}$  is attributed to the B-O stretching of  $[BScB]^-$  anion. Interestingly, this peak is also getting broader and shifted towards higher wavenumber when Li salt is added to the electrolyte. The peak broadness and shift reveal stronger interactions between the  $Li^+$  cations with the  $[BScB]^-$  via oxygen atoms in the anion. The FTIR data suggest that there are higher levels of ion pairing, which might lead to formation of aggregates at higher concentration of lithium salt in the electrolytes. This FTIR data support the findings of NMR spectroscopy.

The combined FTIR and NMR measurements suggested strong interactions between  $Li^+$  cations and  $[BScB]^-$  anions in ionic liquids based hybrid electrolytes. Recently, we have reported that the aromatic  $[BScB]^-$  anion may be coordinated through the delocalized electrons, one oxygen atom or two, and/or may be coordinated to a single  $Li^+$  cation or more<sup>37</sup>. Such interactions lead to ionic clustering at higher concentrations of Li salt in the ionic liquid. Forsyth *et al.* have previously observed similar ionic clustering at higher concentration of NaFSI salt in  $C_3mPyr$  ionic liquid<sup>50</sup>. This work has demonstrated that ionic clustering occurs not only in neat ionic liquid based electrolytes but also in ionic liquid based hybrid electrolytes in the presence of organic solvent.

Figure 11 presents the cyclic voltammograms of  $[P_{4,4,4,8}][BScB]$  IL based hybrid electrolytes at  $20^\circ\text{C}$  temperature. It could evidently be seen that the concentration of Li salt has a remarkable effect on the observed electrochemical behavior of the electrolyte. Generally, the cathodic and anodic limits of the electrolytes are being set by the reduction of cation and oxidation of anion, respectively. The upper anodic limit for all electrolyte reaches  $\sim 6.0\text{ V}$  vs Li and this is the oxidation stability limit of  $[BScB]^-$  anion. The charge delocalization and  $\pi$  conjugated system in  $[BScB]^-$  anionic structure might be the reason of high oxidation potential of the electrolyte. The major variation in the stability of electrolyte is observed at cathodic reduction potential. It has been observed that the

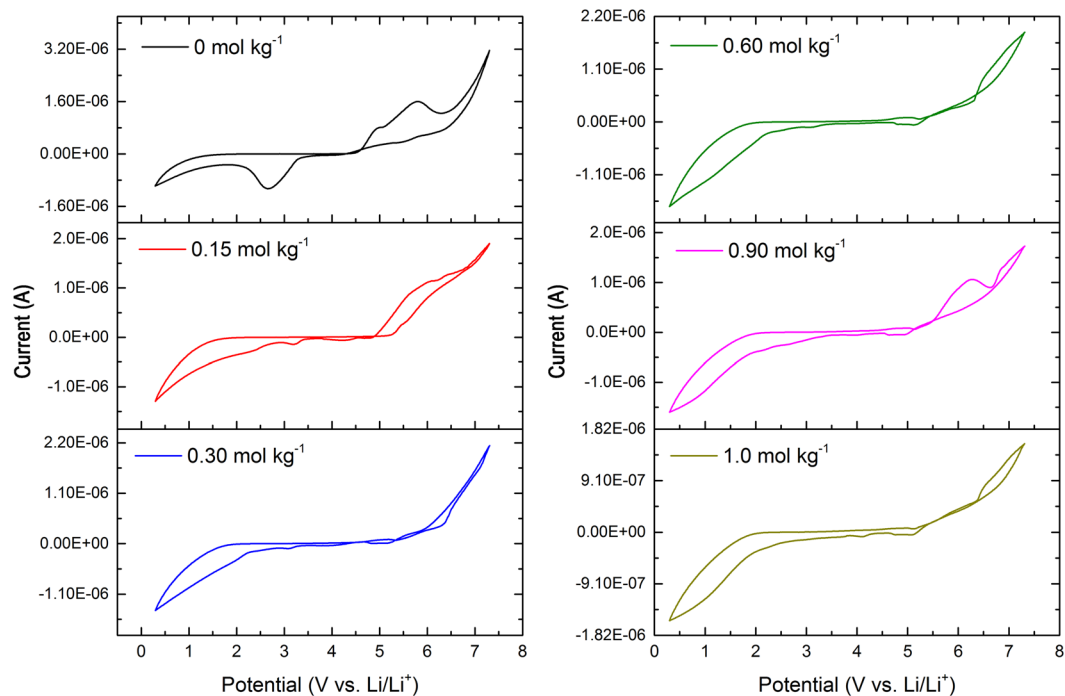


**Figure 11.** Cyclic voltammetry of  $[P_{4,4,4,8}][BScB]$  IL based hybrid electrolytes at 20 °C temperature.

cathodic limit of  $[P_{4,4,4,8}][BScB]$  IL and DEGDBE is slightly suppressed from 1.45 V to 1.55 V vs Li upon addition of  $0.15 \text{ mol kg}^{-1}$  Li[BScB] in the electrolyte. This further decreases to 1.9 V vs Li with the addition of  $1.0 \text{ mol kg}^{-1}$  of Li[BScB] salt. This reduction in cathodic limit might be due to the ion-ion interactions and association of ions in presence of Li salt, which probably leads to decrease in the availability of ions<sup>42</sup>. The electrochemical window of electrolytes was observed in the range of 4.5 to 5 V.

## Conclusions

The ion transport behaviour of halogen-free hybrid electrolytes based on  $[P_{4,4,4,8}][BScB]$  IL mixed with DEGDBE in a 1:5 molar ratio was thoroughly investigated. A maximum solubility of Li[BScB] salt in a mixture  $[P_{4,4,4,8}][BScB]$  and DEGDBE was  $1.0 \text{ mol kg}^{-1}$  at room temperature. The viscosity of the mixture was >1000 times lower as compared with the neat  $[P_{4,4,4,8}][BScB]$  ionic liquid. However, no significant changes are observed in the ionic conductivity of the mixture as compared the neat  $[P_{4,4,4,8}][BScB]$  ionic liquid. As expected, an increase in the ionic conductivity is observed with increase in temperature and a decrease is found with the addition of Li[BScB] salt to the mixture  $[P_{4,4,4,8}][BScB]$  and DEGDBE. The PFG NMR data suggested that the ionic mobility is increasing at increase in temperature and decrease with increasing Li[BScB] concentrations. PFG NMR, liquid state  $^7\text{Li}$  and  $^{11}\text{B}$  NMR and FTIR spectroscopic techniques suggested strong interactions between the lithium cation and the  $[BScB]^-$  anion, which lead to ion association in the electrolytes. This ion association with addition of Li[BScB] salt to the mixture  $[P_{4,4,4,8}][BScB]$  and DEGDBE decreases the mobility of ions as well as the solvent molecules.

## References

- Brennecke, J. F. & Gurkan, B. E. Ionic liquids for CO<sub>2</sub> capture and emission reduction. *J. Phys. Chem. Lett.* **1**, 3459–3464 (2010).
- Etacheri, V., Marom, R., Elazari, R., Salitra, G. & Aurbach, D. Challenges in the development of advanced Li-ion batteries: a review. *Energy Environ. Sci.* **4**, 3243–3262 (2011).
- Xia, L., Yu, L., Hua, D. & Chen, G. Z. Electrolytes for electrochemical energy storage. *Mater. Chem. Front.* **1**, 584–618 (2017).
- Shah, F. U. *et al.* Halogen-free chelated orthoborate ionic liquids and organic ionic plastic crystals. *J. Mater. Chem.* **22**, 6928–6938 (2012).
- Shah, F. U., Glavatskih, S. & Antzutkin, O. N. Boron in tribology: from borates to ionic liquids. *Tribol. Lett.* **51**, 281–301 (2013).
- Wang, Y. L., Shah, F. U., Glavatskih, S., Antzutkin, O. N. & Laaksonen, A. Atomistic insight into orthoborate-based ionic liquids: force field development and evaluation. *J. Phys. Chem. B* **118**, 8711–8723 (2014).
- Giffin, G. A. Ionic liquid-based electrolytes for “beyond lithium” battery technologies. *J. Mater. Chem. A* **4**, 13378–13389 (2016).
- Bayley, P. M. *et al.* Transport properties of ionic liquid electrolytes with organic diluents. *Phys. Chem. Chem. Phys.* **11**, 7202–7208 (2009).
- Vogl, T., Menne, S. & Balducci, A. Mixtures of protic ionic liquids and propylene carbonate as advanced electrolytes for lithium-ion batteries. *Phys. Chem. Chem. Phys.* **16**, 25014–25023 (2014).
- Aguilera, L., Scheers, J. & Matic, A. Enhanced low-temperature ionic conductivity via different Li<sup>+</sup> solvated clusters in organic solvent/ionic liquid mixed electrolytes. *Phys. Chem. Chem. Phys.* **18**, 25458–25464 (2016).
- Giri, S., Behera, S. & Jena, P. Superhalogens as building blocks of halogen-free electrolytes in lithium-ion batteries. *Angew. Chem.* **126**, 14136–14139 (2014).
- Basile, A., Yoon, H., MacFarlane, D. R., Forsyth, M. & Howlett, P. C. Investigating non-fluorinated anions for sodium battery electrolytes based on ionic liquids. *Electrochem. Commun.* **71**, 48–51 (2016).
- Lee, D. J., Hassoun, J., Panero, S., Sun, Y. K. & Scrosati, B. A tetraethylene glycol dimethylether-lithium bis(oxalate)borate (TEGDME-LiBOB) electrolyte for advanced lithium ion batteries. *Electrochem. Commun.* **14**, 43–46 (2012).

14. Zhao, Q. *et al.* Compatibility between Lithium Bis(oxalate)borate-Based Electrolytes and a  $\text{LiFe}_{0.6}\text{Mn}_{0.4}\text{PO}_4/\text{C}$  Cathode for Lithium-Ion Batteries. *Energy Technol.* **5**, 406–413 (2017).
15. Barthel, J., Wuhr, M., Buestrich, R. & Gores, H. J. A new class of electrochemically and thermally stable lithium salts for lithium battery electrolytes: I. synthesis and properties of lithium bis[1,2-benzenediolato(2-)-O,O']borate. *J. Electrochem. Soc.* **142**, 2527–2531 (1995).
16. Barthel, J., Buestrich, R., Carl, E. & Gores, H. J. A new class of electrochemically and thermally stable lithium salts for lithium battery electrolytes: III. synthesis and properties of some lithium organoborates. *J. Electrochem. Soc.* **143**, 3572–3575 (1996).
17. Handa, M., Fukuda, S., Sasaki, Y. & Usami, K. Use of a chelate complex with boron as a lithium salt for lithium battery electrolytes. *J. Electrochem. Soc.* **144**, L235–L237 (1997).
18. Xue, Z. M., Ding, Y. Z. & Chen, C. H. A DFT study of electronic structures, energies, and molecular properties of lithium bis[croconato]borate and its derivatives. *Electrochim. Acta* **53**, 990–997 (2007).
19. Sasaki, Y., Handa, M., Kurashima, K., Tonuma, T. & Usami, K. Application of lithium organoborate with salicylic ligand to lithium battery electrolyte. *J. Electrochem. Soc.* **148**, A999–A1003 (2001).
20. Aurbach, D., Gnanaraj, J. S., Geissler, W. & Schmidt, M. Vinylene carbonate and Li salicylatoborate as additives in  $\text{LiPF}_6(\text{CF}_3\text{CF}_2)_3$  solutions for rechargeable Li-ion batteries. *J. Electrochem. Soc.* **151**, A23–A30 (2004).
21. Swiderska-Mocek, A. & Naparstek, D. Physical and electrochemical properties of lithium bis(oxalate)borate–organic mixed electrolytes in Li-ion batteries. *Electrochimica Acta* **204**, 69–77 (2016).
22. Li, Y. *et al.* A Novel Electrolyte Salt Additive for Lithium-Ion Batteries with Voltages Greater than 4.7 V. *Adv. Energy Mater.* **7**, 1601397 (2017).
23. Xu, K., Zhang, S. S., Lee, U., Allen, J. L. & Jow, T. R. LiBOB: Is it an alternative salt for lithium ion chemistry? *J. Power Sources* **146**, 79–85 (2005).
24. Xu, K., Zhang, S., Poesch, B. A. & Jow, T. R. Lithium bis(oxalato)borate stabilizes graphite anode in propylene carbonate. *Electrochem. Solid-State Lett.* **5**, A259–A262 (2002).
25. Niedzicki, L. *et al.* Lithium cation conducting TDI anion-based ionic liquids. *Phys. Chem. Chem. Phys.* **16**, 11417–11425 (2014).
26. Jankowski, P., Wieczorek, W. & Johansson, P. New boron based salts for lithium-ion batteries using conjugated ligands. *Phys. Chem. Chem. Phys.* **18**, 16274–16280 (2016).
27. Liu, Z., Chai, J., Xua, G., Wang, Q. & Cui, G. Functional lithium borate salts and their potential application in high performance lithium batteries. *Coordination Chemistry Reviews* **292**, 56–73 (2015).
28. Ping, P., Wang, Q., Sun, J., Feng, X. & Chen, C. Effect of sulfites on the performance of LiBOB/ $\gamma$ -butyrolactone electrolytes. *J. Power Sources* **196**, 776–783 (2011).
29. Carbone, L. *et al.* Polyethylene glycol dimethyl ether (PEGDME)-based electrolyte for lithium metal battery. *J. Power Sources* **299**, 460–464 (2015).
30. Fang, S. *et al.* A novel mixture of diethylene glycol diethylether and non-flammable methyl-nonafluorobutyl ether as a safe electrolyte for lithium ion batteries. *J. Mater. Chem. A* **3**, 21159–21166 (2015).
31. Ueno, K. *et al.*  $\text{Li}^+$  solvation and ionic transport in lithium solvate ionic liquids diluted by molecular solvents. *J. Phys. Chem. C* **120**, 15792–15802 (2016).
32. Ueno, K. *et al.*  $\text{Li}^+$  solvation in glyme–Li salt solvate ionic liquids. *Phys. Chem. Chem. Phys.* **17**, 8248–8257 (2015).
33. Ueno, K., Murai, J., Moon, H., Dokko, K. & Watanabe, M. A Design Approach to Lithium-Ion Battery Electrolyte Based on Diluted Solvate Ionic Liquids. *J. Electrochem. Soc.* **164**, A6088–A6094 (2017).
34. Elia, G. A., Bernhard, R. & Hassoun, J. A lithium-ion oxygen battery using a polyethylene glyme electrolyte mixed with an ionic liquid. *RSC Adv.* **5**, 21360–21365 (2015).
35. Karpierz, E. *et al.* A. Bitner-Michalska, W. Wieczorek, Ternary mixtures of ionic liquids for better salt solubility, conductivity and cation transference number improvement. *Scientific Reports* **6**, 35587 (2016).
36. Shah, F. U., Glavatskih, S., MacFarlane, D. R., Forsyth, M. & Antzutkin, O. N. Novel halogen-free chelated orthoborate-phosphonium ionic liquids: synthesis and tribophysical properties. *Phys. Chem. Chem. Phys.* **13**, 12865–12873 (2011).
37. Shah, F. U., Gnezdilov, O. I. & Filippov, A. Ion dynamics in halogen-free phosphonium bis(salicylato)borate ionic liquid electrolytes for lithium-ion batteries. *Phys. Chem. Chem. Phys.* **19**, 16721–16730 (2017).
38. P. T. Callaghan, Principles of nuclear magnetic resonance microscopy; Clarendon; Oxford (1991).
39. Tanner, J. E. Use of the stimulated echo in NMR diffusion studies. *J. Chem. Phys.* **52**, 2523–2526 (1970).
40. Noda, A., Hayamizu, K. & Watanabe, M. Pulsed-gradient spin-echo  $^1\text{H}$  and  $^{19}\text{F}$  ionic diffusion coefficient, viscosity, and ionic conductivity of non-chloroaluminate room-temperature ionic liquids. *J. Phys. Chem. B* **105**, 4603–4610 (2001).
41. Cohen, M. H. & Turnbull, D. Molecular transport in liquids and gases. *J. Chem. Phys.* **31**, 1164–1169 (1959).
42. Plylahan, N., Kerner, M., Lim, D., Matic, A. & Johansson, P. Ionic liquid and hybrid ionic liquid/organic electrolytes for high temperature lithium-ion battery application. *Electrochimica Acta* **216**, 24–34 (2016).
43. Atkins, P. & de Paula, J. Atkins's Physical Chemistry. Oxford University Press. Tenth Ed., 1008 p (2014).
44. Frömling, T., Kunze, M., Schönhoff, M., Sundermeyer, J. & Roling, B. Enhanced lithium transference numbers in ionic liquid electrolytes. *J. Phys. Chem. B* **112**, 12985–12990 (2008).
45. Gélinas, B. *et al.* Electrochemical and transport properties of ions in mixtures of electroactive ionic liquid and propylene carbonate with a lithium salt for lithium-ion batteries. *J. Phys. Chem. C* **120**, 5315–5325 (2016).
46. Martins, V. L., Sanchez-Ramirez, N., Ribeiro, M. C. C. & Torresi, R. M. Two phosphonium ionic liquids with high  $\text{Li}^+$  transport number. *Phys. Chem. Chem. Phys.* **17**, 23041–23051 (2015).
47. Yoon, H., Best, A. S., Forsyth, M., MacFarlane, D. R. & Howlett, P. C. Physical properties of high Li-ion content N-propyl-N-methylpyrrolidinium bis(fluorosulfonyl)imide based ionic liquid electrolytes. *Phys. Chem. Chem. Phys.* **17**, 4656–4663 (2015).
48. Hilder, M. *et al.* Effect of mixed anions on the physicochemical properties of a sodium containing alkoxyammonium ionic liquid electrolyte. *Phys. Chem. Chem. Phys.* **19**, 17461–17468 (2017).
49. Levitt, M. Spin dynamics. Basics of nuclear magnetic resonance (2<sup>nd</sup> Ed); Wiley & Sons; New York (2008).
50. Forsyth, M. *et al.* Novel  $\text{Na}^+$  ion diffusion mechanism in mixed organic–inorganic ionic liquid electrolyte leading to high  $\text{Na}^+$  transference number and stable, high rate electrochemical cycling of sodium cells. *J. Phys. Chem. C* **120**, 4276–4286 (2016).

## Acknowledgements

The Norrbotten Research Council (NoFo) is gratefully acknowledged for the financial support.

## Author Contributions

F.U.S. designed the work, performed most of the experiment and wrote the manuscript. O.I.G. performed PFG NMR measurements. R.G. performed cyclic voltammetry and wrote the text about cyclic voltammetry results. A.F. performed partly the PFG NMR measurements and wrote the diffusivity part of the manuscript. All the authors have read and revised the manuscript before submission.

### Additional Information

**Supplementary information** accompanies this paper at <https://doi.org/10.1038/s41598-017-16597-7>.

**Competing Interests:** The authors declare that they have no competing interests.

**Publisher's note:** Springer Nature remains neutral with regard to jurisdictional claims in published maps and institutional affiliations.



**Open Access** This article is licensed under a Creative Commons Attribution 4.0 International License, which permits use, sharing, adaptation, distribution and reproduction in any medium or format, as long as you give appropriate credit to the original author(s) and the source, provide a link to the Creative Commons license, and indicate if changes were made. The images or other third party material in this article are included in the article's Creative Commons license, unless indicated otherwise in a credit line to the material. If material is not included in the article's Creative Commons license and your intended use is not permitted by statutory regulation or exceeds the permitted use, you will need to obtain permission directly from the copyright holder. To view a copy of this license, visit <http://creativecommons.org/licenses/by/4.0/>.

© The Author(s) 2017